Electronic Supplementary Information for:

High efficiency shear exfoliation for producing high-quality, few-layered MoS_2 nanosheets in a green ethanol /water system

Hong Yuan [a, b], Xiaohong Liu [a, *], Limin Ma [a], Peiwei Gong [a, c], Zhigang Yang [a], Honggang Wang [a], Jinqing Wang [a, *], and Shengrong Yang [a]

[a] State Key Laboratory of Solid Lubrication, Lanzhou Institute of Chemical Physics, Chinese Academy of Sciences, Lanzhou, 730000, P. R. China.

[b] University of Chinese Academy of Sciences, Beijing, 100080, P. R. China

[c] College of Chemistry and Chemical Engineering, Qufu Normal University, Qufu, 273165, P. R. China

* Corresponding authors,
jqwang@licp.cas.cn (J. Wang); xhliu@licp.cas.cn (X. H. Liu)

Fax: +86 931 8277088

Tel.: +86 931 4968076

Figure captions

Fig. S1. FE-SEM images of MoS_2 nanosheets at different magnifications prepared under treating times of 4 h (a, b) and 1 h (c, d).

Fig. S2. (a-f) A series of additional TEM images of MoS_2 nanosheets at different magnifications prepared under treating times of 1, 4, 6, and 10 h, respectively; (g) EDX scan of MoS_2 nanosheets.

Fig. S3. Additional AFM images of typical MoS_2 nanosheets under treating time of 1h.

Fig. S4. XPS survey spectrum and the high resolution XPS O1s spectrum of MoS_2 nanosheets.

Fig. S5. The Reynolds number (*Re*) in ethanol/water system with various volume ratios.

Fig. S6. A Silverson model L5M laboratory high-shear mixer with a D=32 mm mixing head.

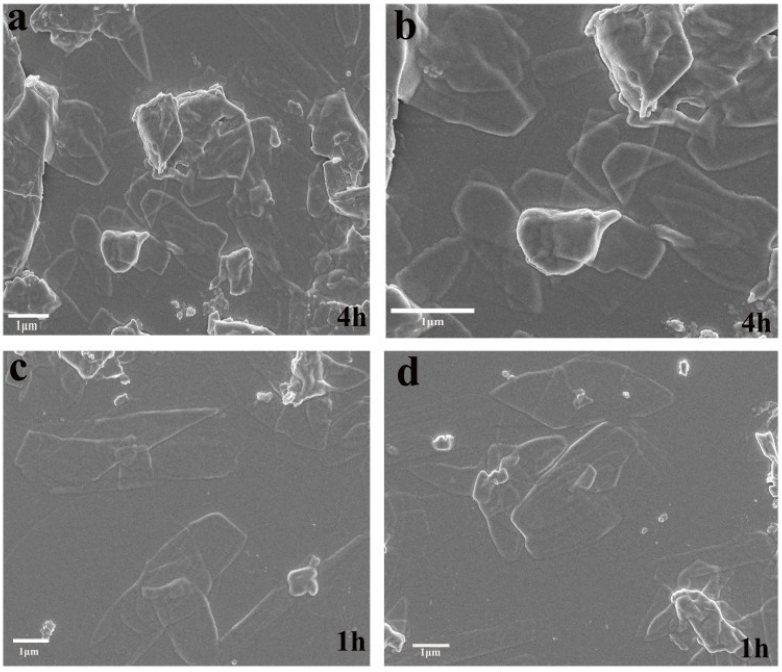

Fig. S1. FE-SEM images of MoS_2 nanosheets at different magnifications prepared under treating times of 4 h (a, b) and 1 h (c, d).

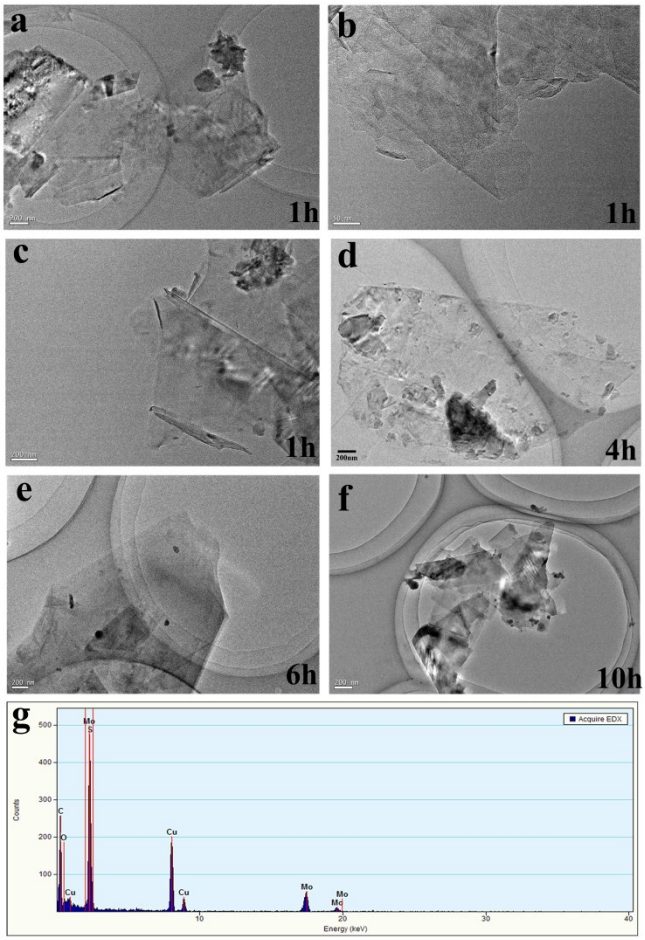

Fig. S2. (a-f) A series of additional TEM images of MoS_2 nanosheets at different magnifications prepared under treating times of 1, 4, 6, and 10 h, respectively; (g) EDX scan of MoS_2 nanosheets.

The FE-SEM and TEM images indicated the morphology of MoS_2 nanosheets with the lateral size from several hundreds of nanometers to several microns. The size of the nanosheets appeared to decrease with prolonging the shear exfoliation time. No impurity peaks appeared in the corresponding EDX scan of MoS_2 on the triangle zone (Cu signals came from TEM grid, which was used to support sample).

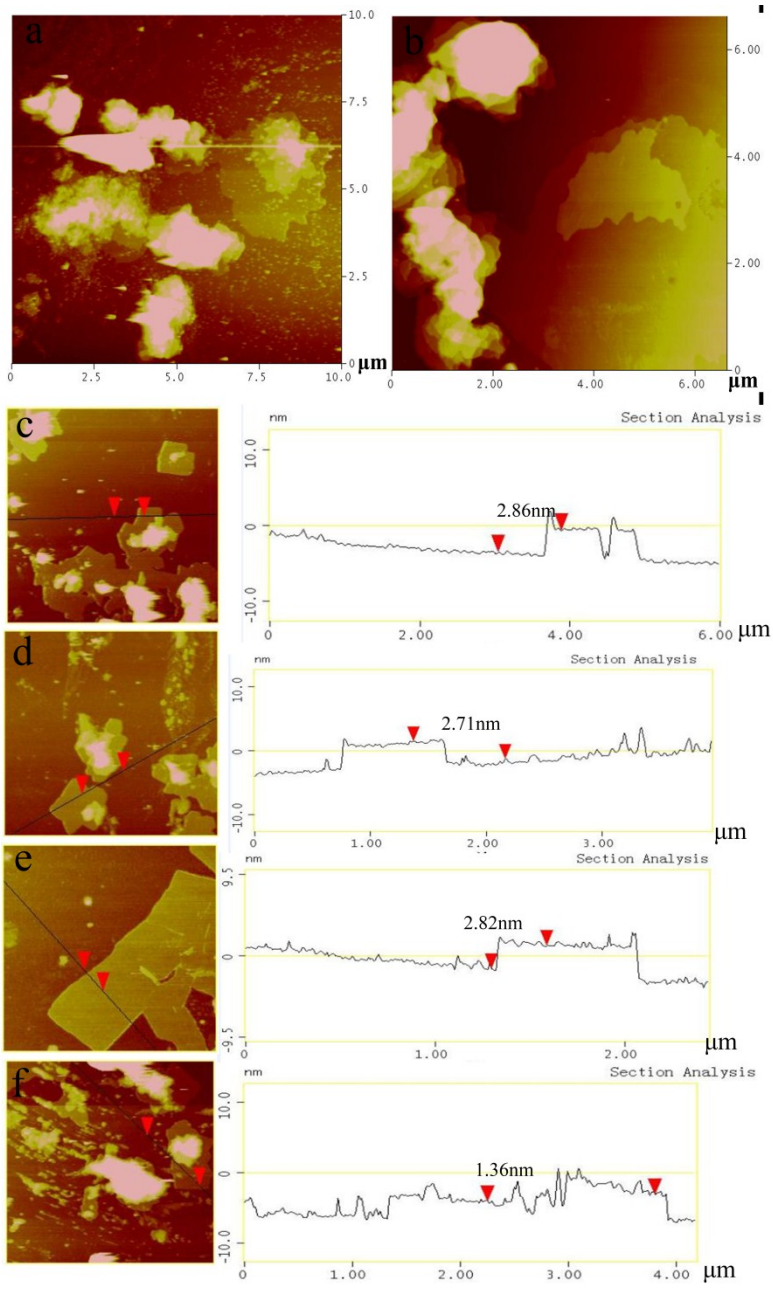

Fig. S3. Some additional AFM images of typical MoS_2 nanosheets under treating time of 1 h

Through these additional AFM images of typical MoS_2 nanosheets, we roughly estimated that the thickness of the nanosheets are mainly in the range of 1.2 to 3 nm, and the local thickness is close to the theoretical value of single layer MoS_2. On the

other hand, the size distribution of the nanosheets can be roughly estimated with the typical lateral size of 0.2~6 μm, which mainly depended on the lateral size of bulk powders (6~40 μm).

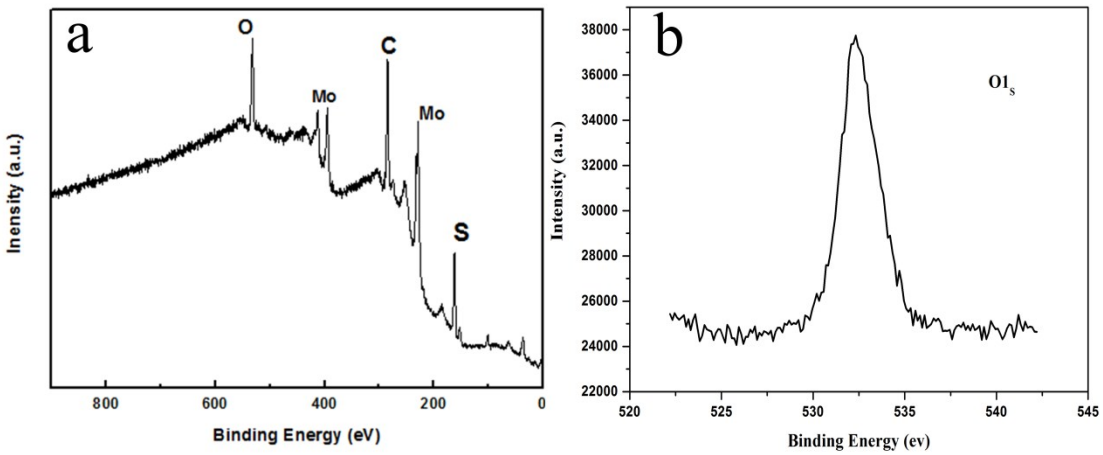

Fig. S4. XPS survey spectrum and the high resolution XPS O1s spectrum of MoS_2 nanosheets.

The XPS survey spectrum revealed that the sample contained the elements of Mo, S, C, and O and the atomic ratio of Mo/S was 1: 2. Two peaks at 229.7 and 232.8 eV in Fig. S4 were attributed to the binding energies of Mo $3d_{5/2}$ and Mo $3d_{3/2}$ for the Mo^{4+} oxidation state. The weak peak at 226.8 eV was assigned to S 2s. The peaks for S 2p were observed at 161.9 and 163.1 eV, corresponding to the S2p $_{3/2}$ and S2p $_{1/2}$ orbits of divalent sulfide ions (S^{2-})[1]. While the peak located at 532.2 eV was consisted with the binding energy of O1s, which was probably attributed to the surface oxidation[2].

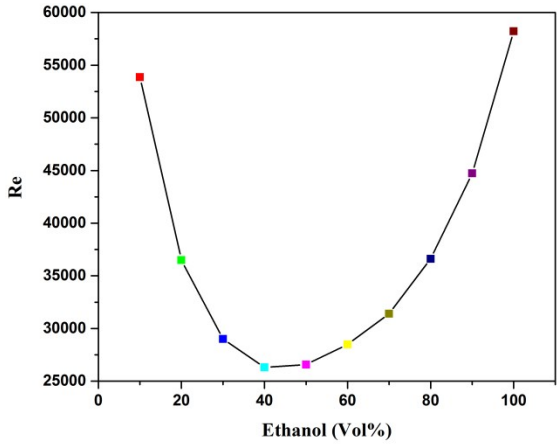

Fig. S5. The Reynolds number (*Re*) in ethanol/water system with various volume ratios.

Generally, the Reynolds number of *Re* is defined as $R_e = \frac{\rho N D^2}{\eta}$, when *Re*>$10^4$, intensive velocity fluctuations in turbulence can induce Reynolds shear stress. Typically, the *Re* in 45 Vol% ethanol aqueous solution: taking the density of ethanol as ~789 kg/m^3, rotational speed N as ~ 10000 rpm=9.6×10^4 rad/s, impeller diameter D as ~32 mm, and dynamics viscosity of 45 Vol% ethanol aqueous solution η as 2.91 m Pa·s (15^{o}C), we can obtain Re≈3×10^4 >10^4. When *Re* >10^4, intensive velocity fluctuations in turbulence can induce Reynolds shear stress[3, 4]. The 45 Vol% ethanol aqueous solution has the minimum *Re*, corresponding to the smallest turbulent friction coefficient[5]. Consistently, the experimental dispersion concentration in the 45 Vol% mixed solvent is the highest, thus the 45 Vol% ethanol aqueous solution system was selected through synthetical consideration.

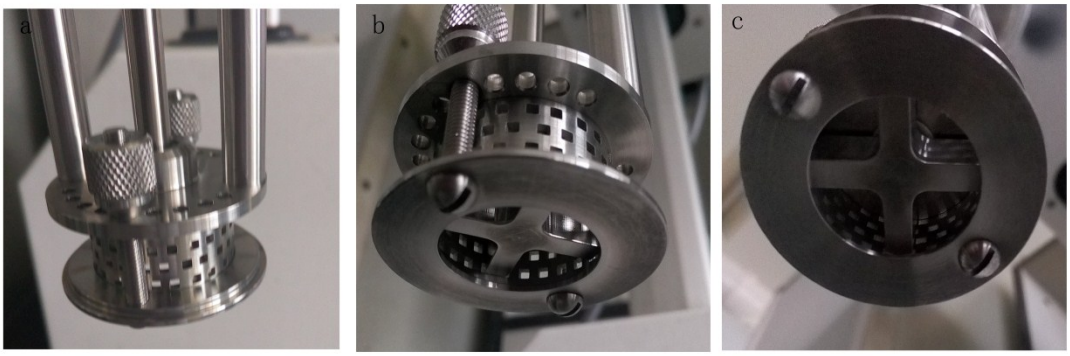

Fig. S6. A Silverson model L5M laboratory high-shear mixer with a D=32 mm mixing head.

Silverson model L5M mixer generates high shear by using a closely spaced (~100 μm) rotor/stator combination. A comprehensive range of heads and screens is available for the Silverson model L5M laboratory high-shear mixer. The high shear mixer has already been widely applied in shear and emulsification. The typical characteristics of the Silverson laboratory high-shear equipment we used are available with a range of rotor diameters which has a narrow gap (~100 μm) between the rotor and stator. It is worth considering that the equipment can generate turbulent shear rate throughout the vessel which is high enough to exfoliate layered compounds[3, 4]. The working mechanisms of the high shear mixer are based on hydrodynamics which can be divided into high shear force, collision effects and jet cavitation[3, 4].The exfoliation occurs in the vortex fluidic shear device which arises from the interplay between centrifugal and shear forces. When the mixing axis revolve around the main frame, the laminas can force materials to writhe up and down and double-knead at the same time, so it can shear efficiently in a short time. Meanwhile, the fluid dynamics events

including random shake and liquid spray could collectively generate viscous shear, turbulence, collision, and pressure to exfoliate mildly bulk counterparts into nanosheets. The partially exfoliated MoS_2 deliberately captured in this process with translational, rotational, lateral shear force as well as collision and jet cavitation at a high rotational speed of 10000 rpm, resulting in the main energy dissipation of the high shear system[5, 6].

These easily interchangeable heads/screens offer great versatility by allowing the machine to be adapted to perform a wide range of mixing operations. The D=32 mm rotor/stator was used in this work and figure S6. (a-c) shows a schematic illustrating the operation of the rotor and stator. This asymmetry is to prevent the formation of a vortex during mixing and ensure bulk circulation of the liquid in the vessel[7]. The mixer speed can be set during operating by tuning the control knob. We initially programmed the mixer to run to a set time of 1 h, at a high speed of 10000 rpm and stop every thirty minutes to avoid overheating during this shear process.

References

1. H. Li, H. Wu, S. Yuan and H. Qian, *Scientific Reports*, 2016, **6**, 21171-21171.

2. L. Tan, S. Wang, K. Xu, T. Liu, P. Liang, M. Niu, C. Fu, H. Shao, J. Yu, T. Ma, X. Ren, H. Li, J. Dou, J. Ren and X. Meng, *Small*, 2016, **12**, 2046-2055.

3. L. Liu, Z. Shen, M. Yi, X. Zhang and S. Ma, *RSC Advances*, 2014, **4**, 36464-36470.

4. K. R. Paton, E. Varrla, C. Backes, R. J. Smith, U. Khan, A. O'Neill, C. Boland, M. Lotya, O. M. Istrate, P. King, T. Higgins, S. Barwich, P. May, P. Puczkarski, I.

Ahmed, M. Moebius, H. Pettersson, E. Long, J. Coelho, S. E. O'Brien, E. K. McGuire, B. M. Sanchez, G. S. Duesberg, N. McEvoy, T. J. Pennycook, C. Downing, A. Crossley, V. Nicolosi and J. N. Coleman, *Nature Materials*, 2014, **13**, 624-630.

5. E. Varrla, C. Backes, K. R. Paton, A. Harvey, Z. Gholamvand, J. McCauley and J. N. Coleman, *Chemistry of Materials*, 2015, **27**, 1129-1139.

6. S. Najmaei, Z. Liu, W. Zhou, X. L. Zou, G. Shi, S. D. Lei, B. I. Yakobson, J. C. Idrobo, P. M. Ajayan and J. Lou, *Nature Materials*, 2013, **12**, 754-759.

7. H. Wadell, *Journal of the Franklin Institute*, 1934, **217**, 459-490.